Holographic aberration correction: optimising the stiffness of an optical trap deep in the sample

Maria Dienerowitz,* Graham Gibson, Richard Bowman and Miles Padgett

SUPA, School of Physics and Astronomy, University of Glasgow, Glasgow G12 8QQ, UK

*maria.dienerowitz@glasgow.ac.uk

Abstract: We investigate the effects of 1st order spherical aberration and defocus upon the stiffness of an optical trap tens of μm into the sample. We control both these aberrations with a spatial light modulator. The key to maintain optimum trap stiffness over a range of depths is a specific non-trivial combination of defocus and axial objective position. This optimisation increases the trap stiffness by up to a factor of 3 and allows trapping of 1μm polystyrene beads up to 50μm deep in the sample.

OCIS codes: (090.1000) Aberration compensation; (140.7010) Laser trapping; (230.6120) Spatial light modulators; (350.4855) Optical tweezers or optical manipulation.

References and links

1. M. Reicherter, T. Haist, E. Wagemann, and H. Tiziani, "Optical particle trapping with computer-generated holograms written on a liquid-crystal display," Opt. Lett. **24,** 608–610 (1999).
2. J. Curtis, B. Koss, and D. Grier, "Dynamic holographic optical tweezers," Opt. Commun. **207,** 169–175 (2002).
3. M. Padgett and R. Di Leonardo, "Holographic optical tweezers and their relevance to lab on chip devices," Lab Chip **11,** 1196–1205 (2011).
4. K. Wulff, D. Cole, R. Clark, R. Di Leonardo, J. Leach, J. Cooper, G. Gibson, and M. Padgett, "Aberration correction in holographic optical tweezers," Opt. Express **14,** 4170–4175 (2006).
5. A. Jesacher, A. Schwaighofer, S. Fürhapter, C. Maurer, S. Bernet, and M. Ritsch-Marte, "Wavefront correction of spatial light modulators using an optical vortex image," Opt. Express **15,** 5801–5808 (2007).
6. R. Bowman, A. Wright, and M. Padgett, "An SLM-based Shack-Hartmann wavefront sensor for aberration correction in optical tweezers," J. Opt. bf 12, 124004 (2010).
7. I. Vellekoop and A. Mosk, "Focusing coherent light through opaque strongly scattering media," Opt. Lett. **32,** 2309–2311 (2007).
8. T. Čižmár, M. Mazilu, and K. Dholakia, "In situ wavefront correction and its application to micromanipulation," Nature Photon. **4,** 388–394 (2010).
9. E. Theofanidou, L. Wilson, W. Hossack, and J. Arlt, "Spherical aberration correction for optical tweezers," Opt. Commun. **236,** 145–150 (2004).
10. G. Sinclair, P. Jordan, J. Leach, M. Padgett, and J. Cooper, "Defining the trapping limits of holographical optical tweezers," J. Mod. Opt. **51,** 409–414 (2004).
11. S. Reihani, M. Charsooghi, H. Khalesifard, and R. Golestanian, "Efficient in-depth trapping with an oil-immersion objective lens," Opt. Lett. **31,** 766–768 (2006).
12. S. Reihani and L. Oddershede, "Optimizing immersion media refractive index improves optical trapping by compensating spherical aberrations," Opt. Lett. **32** 1998–2000 (2007).
13. C. Sheppard and M. Gu "Aberration compensation in confocal microscopy," Appl. Opt. **30,** 3563–3568 (1991).
14. Y. Huang, J. Wan, M. C. Cheng, Z. Zhang, S. M. Jhiang, and C. H. Menq, "Three-axis rapid steering of optically propelled micro/nanoparticles," Rev. Sci. Instrum. **80,** 063107 (2009).
15. R. Bowman, G. Gibson, and M. Padgett, "Particle tracking stereomicroscopy in optical tweezers: Control of trap shape," Opt. Express **18,** 11785–11790 (2010).

#152832 - $15.00 USD Received 15 Aug 2011; revised 25 Oct 2011; accepted 27 Oct 2011; published 16 Nov 2011

16. G. Gibson, J. Leach, S. Keen, A. Wright, and M. Padgett, "Measuring the accuracy of particle position and force in optical tweezers using high-speed video microscopy," Opt. Express **16,** 14561–14570 (2008).
17. A. Rohrbach, and E. Stelzer, "Trapping forces, force constants, and potential depths for dielectric spheres in the presence of spherical aberrations," Appl. Opt. **41,** 2494–2507 (2002).
18. P. Ke and M. Gu, "Characterization of trapping force in the presence of spherical aberration," J. Mod. Opt. **45,** 2159–2168 (1998).
19. C. Sheppard and C. Cogswell, "Effects of aberrating layers and tube length on confocal imaging properties," Optik **87,** 34–38 (1991).

1. Introduction

Holographic tweezers extend the capabilities of standard single beam tweezers allowing one to trap many particles simultaneously as well as offering a wealth of beam-shaping options [1, 2]. Optimising the stiffness of the optical trap is crucial for a range of applications such as trapping nanoparticles, reducing laser damage in biological samples and minimising the required power for creating complex optical landscapes [3]. Research investigating aberration correction based on a spatial light modulator (SLM) includes correcting for system intrinsic aberrations like astigmatism [4–6] and optimising beam quality for focusing through turbid media [7, 8].

The ability to trap deep within a sample is essential to continue optical tweezers' success as a tool for nanotechnology. The effects of aberrations are more significant when trapping particles smaller than the wavelength of the beam, which make them particularly important for nanoparticle trapping [4]. Beam aberrations are predominantly introduced at the glass-water interface in the sample [9]. Due to the microscope objective's design criteria the optimum focus and thus optical trap is formed a few microns into the sample. To achieve trapping beyond this restricted region, recent work has investigated the effects of defocusing the trapping beam and changing the refractive index of the immersion oil [10–12], applying methods developed for confocal microscopy [13]. In addition to shifting the laser focus axially with an SLM or by moving the tube lens, previous experiments explored the potential of a deformable mirror, which offers the benefit of high bandwidths [9, 14].

In this paper we demonstrate how to maintain the stiffest trap over a range of depths with the aberration correction capabilities of the SLM. The SLM-based correction gives us the advantage of directly examining the effect of spherical aberrations on trap stiffness. Furthermore, the experimental system remains unchanged without having to mechanically adjust lens positions. Based on earlier work [12, 13] we expected that optimizing the 1st order spherical aberrations would allow us to achieve optimum trapping for a range of depths. However, it appears that defocusing the trapping laser is the more important parameter rather than 1st order spherical aberration correction.

2. Experiment

The experimental system combines a standard holographic tweezers setup with a custom stereoscopic microscope [15] enabling 3D particle tracking (see Fig. 1). The holographic tweezers are based on a 100x Nikon objective (CFI Plan Fluor, oil immersion, NA 0.5-1.3) and an x-y stage (ASI MS-2000) with an integrated z stage to position the focus height by moving the objective lens. A cw Ti:Sapphire laser (M Squared, SolsTiS) provides the trapping beam with wavelengths tunable from 790nm to 850nm. We expand the laser beam to fill the active region of a spatial light modulator (Boulder Nonlinear Systems, XY Series, 512x512 pixels) which we subsequently image onto the back aperture of the trapping objective (similar to the system described in [16]). With our stereo imaging system [15] we extract 3D position distributions of a trapped particle from its two 2D video images recorded with a single high speed camera (Prosilica GE680C).

#152832 - $15.00 USD Received 15 Aug 2011; revised 25 Oct 2011; accepted 27 Oct 2011; published 16 Nov 2011

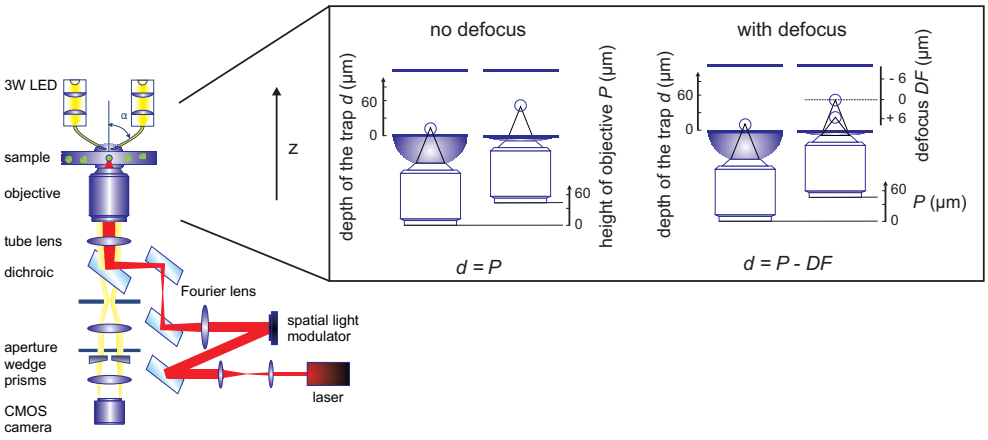

Fig. 1. The left diagram shows the holographic tweezers with the stereo imaging system. The inset clarifies the coordinate system used throughout our experiments. The trapping depth d results from a combination of objective position P and SLM defocus setting DF. The latter is positive if the laser focus is shifted towards the objective and negative for an axial shift away from the objective.

It has been noted by many works in the field [10, 17] that beam aberrations degrade the axial trap stiffness more than the lateral one. Therefore we monitor the axial trap stiffness κ_z by measuring the standard deviation σ_z of the trapped particle's position distributions. The trap stiffness is inversely proportional to σ_z^2. We estimate the error of tracking the position within a single frame as 4-5nm in each direction, which is 2-3 orders of magnitude smaller than the residual Brownian motion of the particle in the trap. We trap 1μm diameter polystyrene spheres suspended in water. This particle size is small enough to help us predict trapping properties for nanoparticle trapping and at the same time large enough to scan an extended parameter space without losing trapping capabilities. For each set of parameters consisting of specific values for astigmatism, defocus and 1st order spherical aberration we measured σ_z as a function of trap depth d in the sample.

3. Results

Despite the flexibility of an SLM, its optical flatness is typically around 1λ. As a result we observed a slight astigmatism of the order of 1λ with an orientation matching the SLM aperture. Figure 2 shows the particle's axial position distribution before and after the astigmatism correction. Interestingly, the effect of astigmatism almost goes unnoticed in the particle's lateral motion but appears in the x-z scatterplot. The standard deviation in z almost halved after the astigmatism correction while the standard deviation in x and y decreased by 20%. The scatterplots are taken with the particle trapped 12μm deep in the sample. We maintained this astigmatism correction throughout all our subsequent experiments.

The main aim of our investigation is to determine how to move the optimum trap position over a considerable range of depths. Our first experiment measured the effect of changing the 1st order spherical aberration on σ_z. The SLM enables us to control the 1st order spherical aberration by adding the appropriate Zernike mode to the hologram displayed on the SLM. Figure 3 shows the standard deviation of the particle's axial position distribution σ_z as a function of the depth d of the trapping focus. The trap stiffness slightly improved by setting the 1st order spherical aberration Zernike coefficient to -0.5, corresponding to a correction of the order of 1λ. However this optimisation was only apparent for one specific trapping depth.

#152832 - $15.00 USD Received 15 Aug 2011; revised 25 Oct 2011; accepted 27 Oct 2011; published 16 Nov 2011

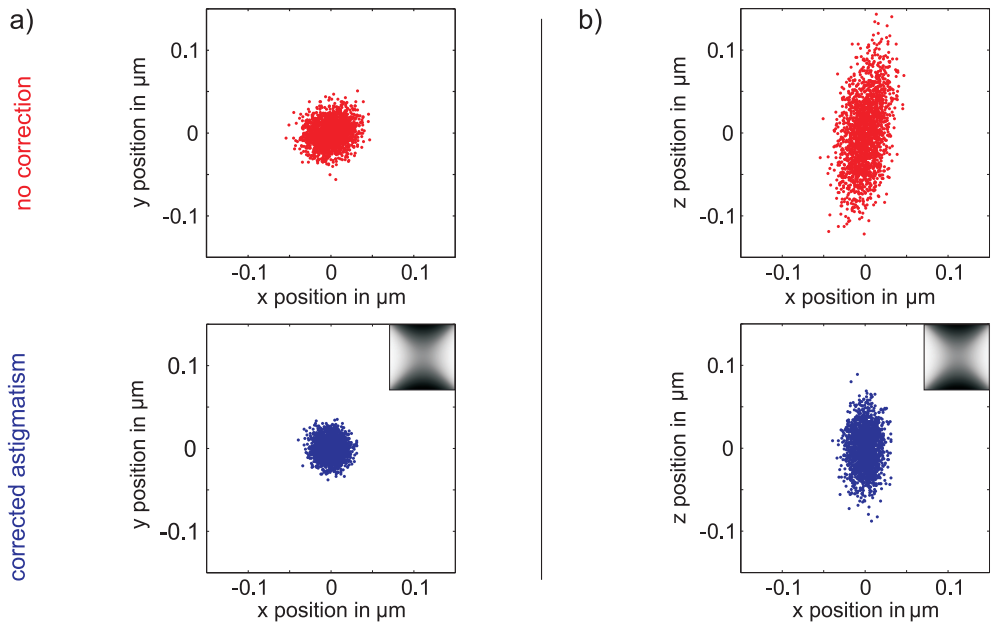

Fig. 2. a) The lateral position distribution of the trapped bead contracts with astigmatism correction which increases the lateral trap stiffness by a factor of 1.6. b) The astigmatism is more obvious in the axial position distribution of the same trapped particle. The improvement in axial trap stiffness is 5 times higher compared to the improvement in lateral direction. The two insets show the hologram displayed on the SLM.

The minimum σ_z in Fig. 3 does not remain constant for varying the 1st order spherical aberration settings. This demonstrates that it is not possible to maintain the optimum trap stiffness over a range of depths by optimising 1st order spherical aberrations alone. Furthermore we experimented with both, standard microscope immersion oil with $n_{standard} = 1.518$ and higher index immersion oil $n = 1.56$ (Cargille Labs). As previously reported [12], using a higher index immersion oil provides a stiffer trap. If the primary effect of the oil is altering the 1st order spherical aberrations, we should have been able to compensate for the change in oil by adjusting the 1st order spherical aberrations. Again, our results show that we are not able to recover the trapping performance for the standard immersion oil by optimising 1st order spherical aberrations only. This suggests that we either have to include higher orders of spherical aberrations [13] or simply optimise another parameter. As the defocus of the microscope objective plays an important role for trapping performance [11], we chose to explore this parameter further.

The next set of experiments investigated the effect of defocus. Instead of mechanically moving the tube lens, we adjusted the Zernike mode for defocus on the SLM. The main advantage of using the SLM is that the beam size at the entrance pupil of the objective then remains unchanged regardless of the amount of defocus. Changing the defocus on the SLM to move the focus axially is one method to shift the optical trap to a different depth. The other is to move the objective stage with respect to the sample. Both scenarios are illustrated in Fig. 1. We show in this paper that these two methods have to be combined to give the optimum trap at a range of depths. For each value of defocus DF we scanned a range of objective positions P and measured the trap stiffness at a depth d in the sample. In our experiment $DF < 0$ means the beam enters the trapping objective diverging and for $DF > 0$ the beam converges prior to the objective. To

#152832 - $15.00 USD Received 15 Aug 2011; revised 25 Oct 2011; accepted 27 Oct 2011; published 16 Nov 2011

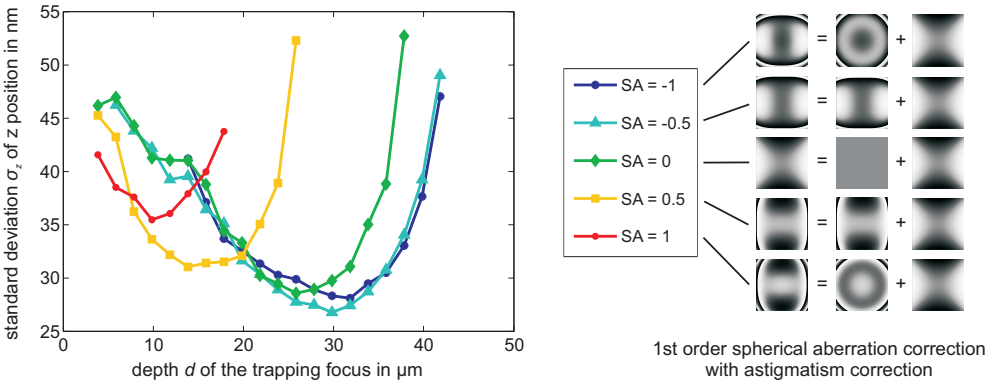

Fig. 3. We plot the standard deviation σ_z of the trapped particle's axial position distribution as a function of trapping depth d. The depth of the optimum trap shifts when changing the amount of spherical aberration (SA) applied, however the trap stiffness decreases for any Zernike coefficient other than -0.5. The right column explains the hologram composition displayed on the SLM. In this experiment we combine astigmatism and spherical aberration correction.

trap a particle at a specific d we have two possible combinations: move the objective towards d and shift the focus the remaining depth up to $d = P + |DF|$ or move the objective past the desired depth and pull the focus back, $d = P - DF$. We found the former provided optimum trapping for depths smaller than the neutral focus position $(DF = 0)$ and the latter proved best for trapping deeper than $DF = 0$, agreeing with previous investigations [11].

We performed measurements with two different immersion oils ($n_{standard} = 1.518$ and $n = 1.56$) and compare our results of the depth scans in Fig. 4. The graphs show the variation of the axial standard deviation σ_z with respect to the defocus setting DF and the trapping depth d. The standard deviation is colour coded with blue representing the lowest values of σ_z and therefore the strongest trap. Trapping with the standard oil is almost impossible for $DF = 0$. However, by moving the objective closer to the sample and pulling the focus back towards the objective we were able to improve the trap stiffness by a factor of 2 and achieve a trap almost as stiff as we obtained using the higher index oil. For example, moving the objective 22μm up and pulling the focus back towards the objective by 6μm positions the optimum trap 16μm deep into the sample. Additionally, we maintained this optimum trap stiffness over a range of 18μm.

The optimum trap for the higher index oil with $DF = 0$ is 18μm into the sample. We shifted the optimum trap in both directions, towards the bottom of the sample as well as deeper into the sample. With a neutral defocus setting trapping is possible up to 32μm in the sample, however with the correct combination of P and DF the trap stiffness at 32μm increased by a factor of 3.5. We shifted the optimum trap throughout the sample over a depth of 30μm without substantially reducing the trap stiffness. For clarity we show the data set comprising the points a)-c) in Fig. 4 in more detail in Fig. 5. Each σ_z originates from a position distribution of a trapped particle. Figure 5 displays these positions of a particle trapped 30μm deep in the sample for DF settings of a) 0μm (σ_z=60.3nm), b) 2μm (σ_z=31.4nm) and c) 4μm (σ_z=25.3nm). The improvement in trap stiffness is a direct result of the improved confinement of the trapped particle in the axial direction.

#152832 - $15.00 USD Received 15 Aug 2011; revised 25 Oct 2011; accepted 27 Oct 2011; published 16 Nov 2011

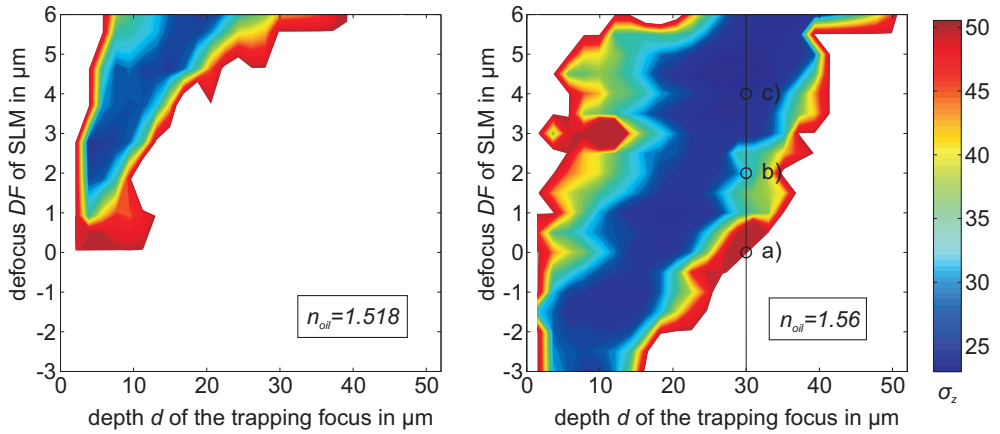

Fig. 4. We compare the trap stiffness for two different immersion oils over a range of defocus settings DF and trapping depths d. The standard deviation σ_z of the particle's axial positions are colour coded. We move the optimum trap (dark blue region) axially by combining defocus DF and objective height P which gives the trapping depth d. The data corresponding to positions a)-c) in the right graph are displayed in more detail in the next figure.

4. Discussion

Our results show that shifting the optimum trap over a range of depths is not achieved by compensating for 1st order spherical aberrations alone but by a combination of defocus and objective height. A frequently cited equation in this context [12, 18] is the wavefront aberration introduced by a slab of dielectric [19]

$$\Delta\phi = k_0\, t(n_2\cos\theta_2 - n_1\cos\theta_1) \tag{1}$$

with $k_0 = 2\pi/\lambda$, the slab thickness t, ray angle in the first medium θ_1 with refractive index n_1 and the dielectric slab n_2. This equation describes the angle dependent total phase change consisting of spherical aberrations and other terms. Expanding this expression in terms of $\sin(\theta_1/2)$ reveals the individual aberration terms more clearly:

$$\Delta\phi = kt(n_2-n_1)\Big(1+\underbrace{2\frac{n_1}{n_2}\sin^2(\frac{\theta_1}{2})}_{\text{defocus}}+\underbrace{2(n_2+n_1)\frac{n_1^2}{n_2^3}\sin^4(\frac{\theta_1}{2})}_{1^{\text{st}}\text{order spherical aberrations}}+O(\sin^6(\theta_1/2))\Big) \tag{2}$$

The first term is an overall phase change, independent of angle, the second term is attributed to defocus and the third to 1st order spherical aberrations. Defocus is the dominant term for our experimental conditions at the oil-glass interface $(\theta_1 = 60°, n_1 = 1.518, n_2 = 1.56)$ and the glass-water interface $(\theta_1 = 60°, n_1 = 1.518, n_2 = 1.33)$. A similar equation exists for the effect of the tube lens [19]. Both equations support our findings that the effect of defocus on the total phase change is more important than the effect of 1st order spherical aberration alone.

The phase changes at the glass-water interface is the most significant and has a negative sign. Changing the defocus to introduce a positive phase change compensates for this. Evidently this compensation adjusts any phase aberrations introduced by defocus as well as minimising spherical aberrations. Expanding the equation for the effect of the tube lens [19] in terms of $\sin(\theta_1/2)$, the leading order is approximated by $\Delta\phi = 2k_0\, n_{water}\, d' sin^2\frac{\theta_1}{2}$ with d' the depth of

#152832 - $15.00 USD Received 15 Aug 2011; revised 25 Oct 2011; accepted 27 Oct 2011; published 16 Nov 2011

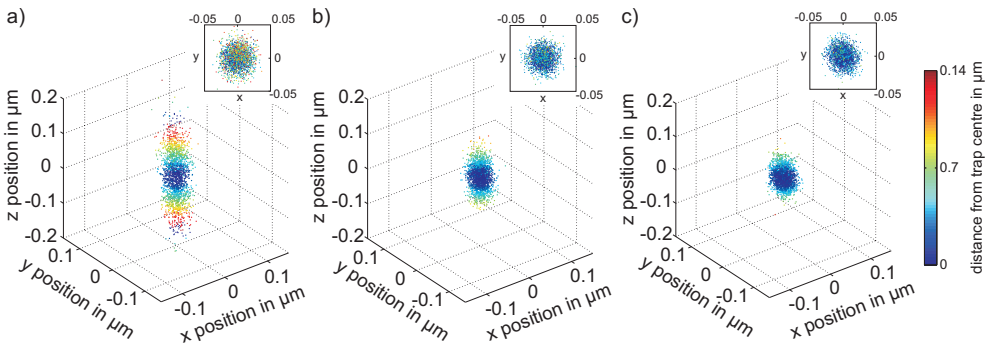

Fig. 5. We compare the position distribution of a particle trapped 30μm deep in the sample with defocus settings of a) 0μm, b) 2μm and c) 4μm. As indicated by the standard deviation values in Fig. 4, the trap strength increases for increasing defocus resulting in a contracted position distribution. The colour of the data point corresponds to the radial distance from the trap centre. The insets show the same data in a top view (x-y-plot) and demonstrate that the improvement in trap stiffness by more than a factor of 2 is most obvious in the z direction.

the focus. This term is positive for our experimental configuration and thus compensates for negative phase changes at the glass-water interface described in Eq. (2).

5. Conclusion

We trapped 1μm polystyrene spheres up to 50μm deep in the sample and maintained the optimum trap stiffness over the entire range of depths in our experiments. Additionally we achieved comparable trap stiffness for standard and high index immersion oil. The key to optimising the optical trap deep in the sample is a specific combination of objective position and defocus. The deeper we want to trap the further we have to move the objective up and pull the focus back again. For example to trap 32μm deep, we moved the objective 38μm up and pulled the focus 6μm back towards the objective. This improved the trap stiffness by a factor of 3 compared to moving the objective only. For comparison - optimising 1st order spherical aberrations alone only increased the trap stiffness by a factor of 1.14. The holographic implementation of the SLM proved ideal as any change in aberration correction setting is instantly reversible and does not require any mechanical adjustments. Our results can easily be implemented in other holographic tweezers systems.

#152832 - $15.00 USD Received 15 Aug 2011; revised 25 Oct 2011; accepted 27 Oct 2011; published 16 Nov 2011